* I find that observable very interesting in context of experimental studies as measurement of neutron at E ≈ 70 MeV is nowadays within our reach.

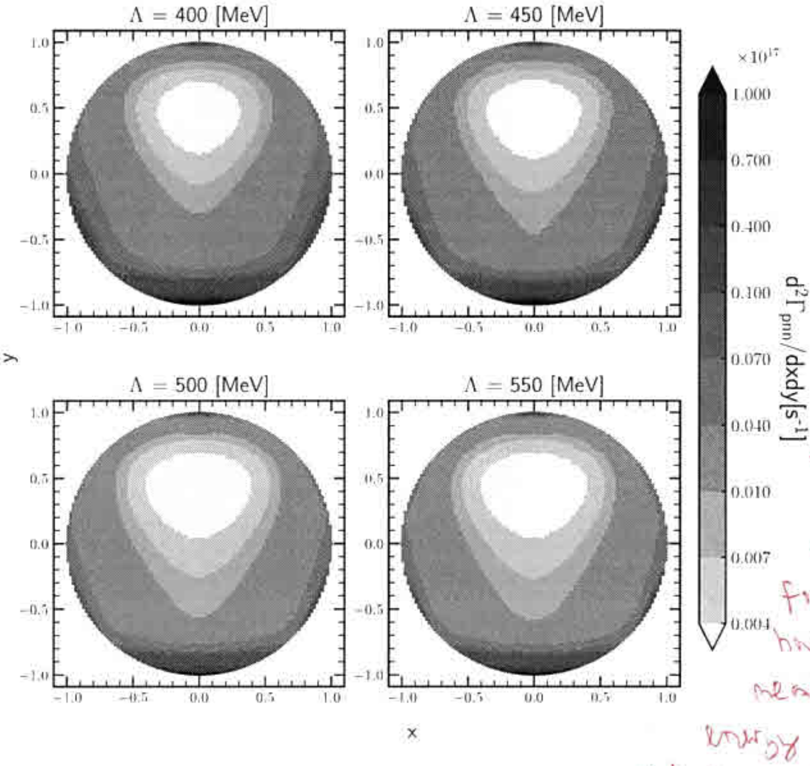

That observable could be an interesting experimental test for the cut-off value, however it requires measurement at low proton energy (~0.8-1.0 MeV) which is an experimental challenge.

Figure 3.53: The same as in Fig. 3.52 but for the double differential absorption rates $d^2\Gamma_{pnn}/dxdy$.

The right panel of the Fig. 3.60 shows a cut-off dependance of the predictions obtained with the SMS chiral potential at N^{4}LO$^+$. In this case maximum point is interesting as well. We see that predictions with Λ = 500 MeV and 550 MeV are quite close to each other: the relative difference between them at E$_p$ = 0.92 MeV is only 1.5 %. In turn the spread between Λ = 400 MeV, 450 MeV and 500 MeV is 40 % (at the same ~~point~~). This cut-off dependance is hidden looking at the colormaps Fig. 3.52, but from this prospective it is clearly presented. Anyway, the highest Λ, the biggest dΓpnn/dEp is seen.

Similarly in Fig. 3.61 $d\Gamma_{pnn}/dE_n$ is presented. We observe similar trends which are also shown up at the ~~extremum~~ point which is around E$_n$ = 66.9 MeV now. The difference between N^{2}LO and N^{4}LO$^+$ predictions at this point is 29.0 %. The relative difference between all the predictions except for N^{2}LO is 7.5 %. The ~~cut-off~~ predictions are also very similar for Λ = 500 MeV and 550 MeV (the spread is 1.6 %) while all ~~the rest~~ predictions are quite distinguished - the spread is 39.1 %. *

~~Coming~~ to the next figures, Fig. 3.62 and Fig. 3.63, ~~which~~ show ~~1D~~ dependance of the absorption rate on the Dalitz coordinates $r = \sqrt{x^2 + y^2}$ and $\phi = \arctan \frac{y}{x}$. The similar trend is preserved, namely chiral order figures show that N^{2}LO predictions outstand from all other predictions, and noticeable cut-off dependance is observed.

In general we can conclude that predictions are converged starting from the N^{3}LO chiral order as most of the demonstrated results show that the difference between N^{3}LO, N^{4}LO and N^{4}LO$^+$ is negligible. At the same time we observe a cut-off dependance ~~where~~ predictions obtained with Λ = 500 MeV and 550 MeV ~~are~~ very similar, but ~~the~~ spread ~~with~~ all the rest ~~values is there~~. This nature of the cut-off dependance is also reflected in the total absorption rate, presented in Fig. 3.49.

results   strong   with big   (for NN force)

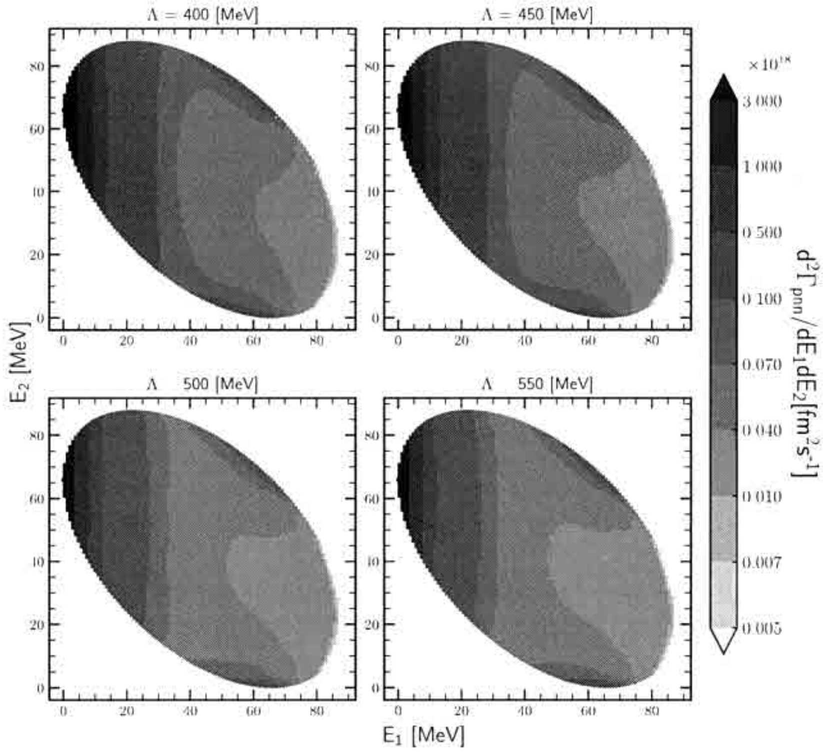

supplemented by N²LO 3NF

NN

Figure 3.54: Intensity plots for the double differential absorption rates $d^2\Gamma_{pnn}/dE_1dE_2$ for the $\pi^- +^3$ He $\rightarrow p + n + n$ process, obtained using the SMS potential at N^{4}LO$^+$ with plane wave part only (without rescattering). All other contributions are the same as in Fig. 3.52: 1NC + 2N and 2NF+3NF. Each panel present predictions obtained with different values of the cut-off parameter Λ: from 400 MeV (upper left) to 550 MeV (lower right). Nucleon 1 is a proton.

$\Lambda =$ $\Lambda =$

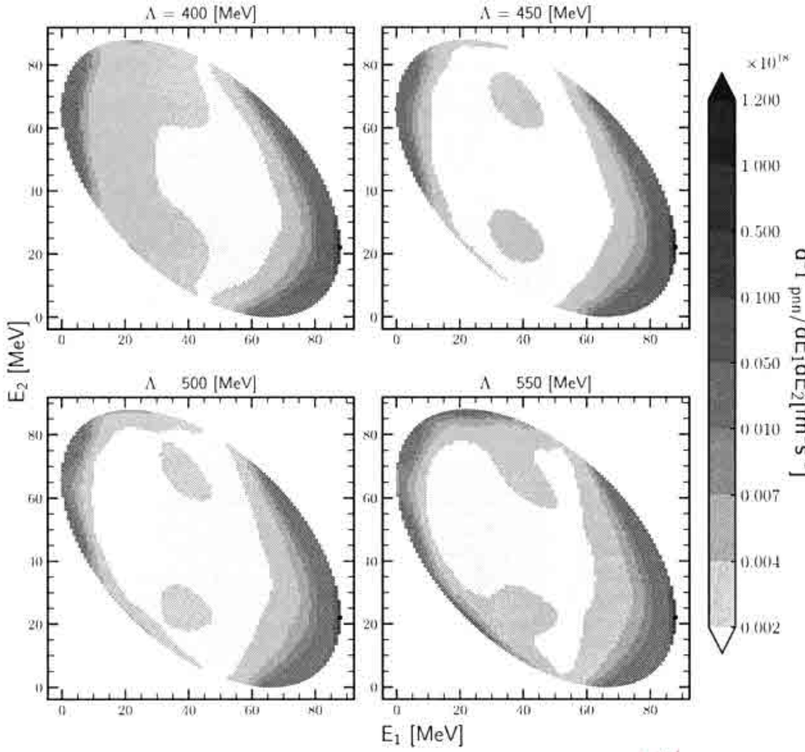

currents

/NN

supplemented by the N^{2}LO 3NF

Figure 3.56: Intensity plots for the double differential absorption rates $d^2\Gamma_{pnn}/dE_1dE_2$ for the $\pi^- + {}^3\mathrm{He} \to p + n + n$ process, obtained using the SMS potential at N^{4}LO$^+$ with 1NC only (without 2N). All other contributions are the same as in Fig. 3.52: PWIAS+RESC and 2NF+3NF. Each panel presents predictions obtained with different values of the cut-off parameter Λ: from 400 MeV (upper left) to 550 MeV (lower right). Nucleon 1 is a proton.

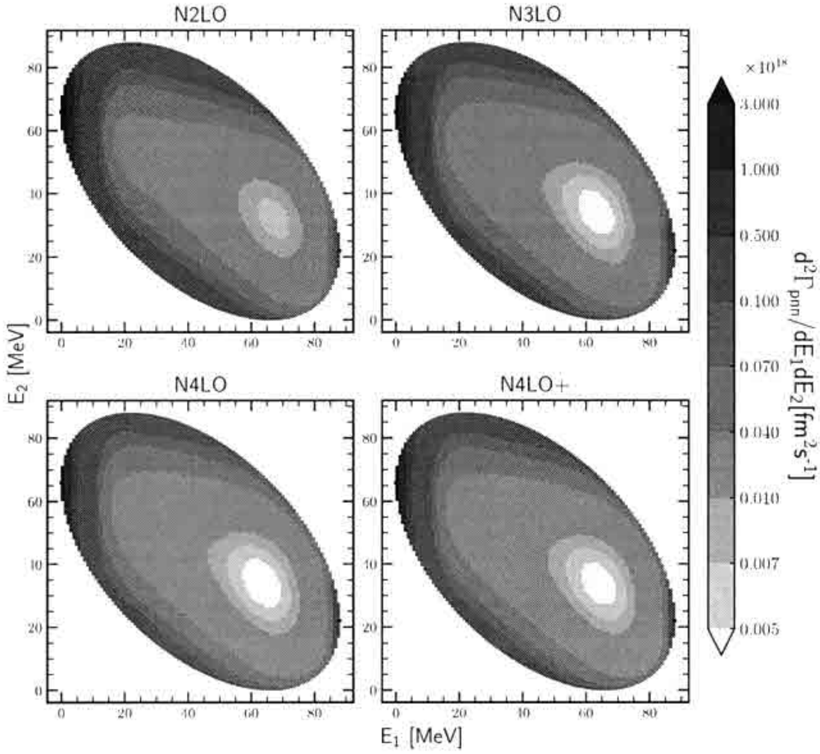

Figure 3.58: Intensity plots for the double differential absorption rates $d^2\Gamma_{pnn}/dE_1dE_2$ for the $\pi^- +^3$ He $\rightarrow p + n + n$ process, obtained using the SMS potential ~~at N⁴LO⁺~~ with all contributions possible: plane wave + rescattering, 1NC + 2N, 2NF+3NF. Each panel presents predictions obtained with different chiral orders of the SMS potential: from $\mathrm{N}^2\mathrm{LO}$ (upper left) to $\mathrm{N}^4\mathrm{LO}^+$ (lower right) and with $\Lambda = 450$ MeV. Nucleon 1 is a proton.

3NF was taken at $\mathrm{N}^2\mathrm{LO}$ in each case.

NN

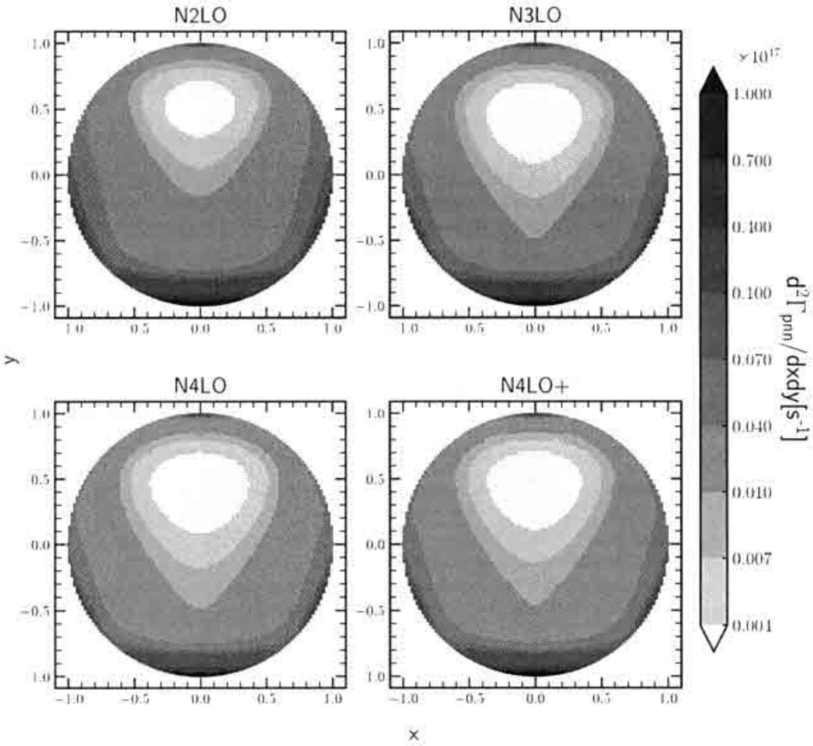

Figure 3.59: The same as in Fig. 3.58 but for the double differential absorption rates $d^2\Gamma_{pnn}/dxdy$.

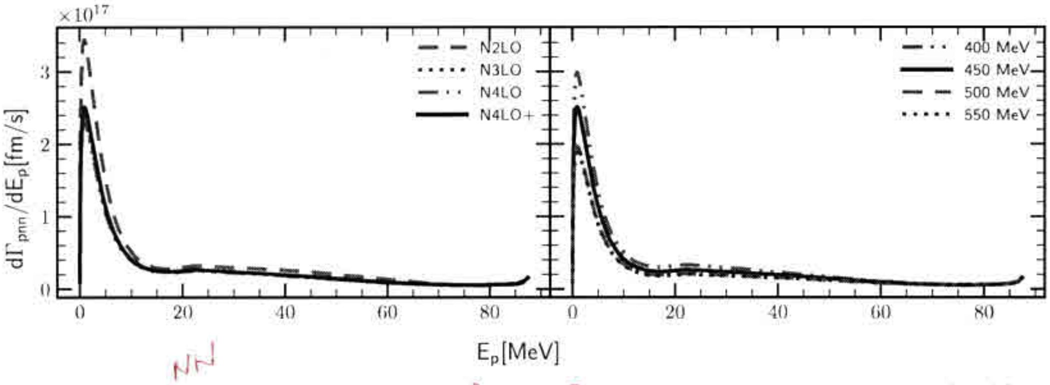

NN

plus N²LO 3NF

the NN

Figure 3.60: Differential absorption rate $d\Gamma_{pnn}/dE_p$ as a function of the proton energy E_p for the $\pi^- + 3He \rightarrow p + n + n$ process. Left panel shows results obtained with N^{2}LO (green dashed line), N^{3}LO (blue dotted line), N^{4}LO (red dashed-double-dotted line) and N^{4}LO$^+$ (black solid line) chiral orders, and with $\Lambda = 450\,$MeV. The right panel includes results obtained with the N^{4}LO$^+$ SMS potential with different values of the Λ: 400 MeV (red dashed-double-dotted line), Λ: 450 MeV (black solid line), Λ: 500 MeV (green dashed line line) and Λ: 550 MeV (blue dotted line). All predictions were obtained with "FULL-(1NC+2N)-(2NF+3NF)" setup.

NN

Γ_{nnn} for that process

is allowed

dynamical model

~~count~~ ok

3.4.3 Pion absorption in ^{3}H

In this subsection I will show results of calculations for the $\pi^- + {}^3\mathrm{H} \to n + n + n$ process. In this case ~~we have~~ only a three-body breakup as no two-body configuration can be composed out of three neutrons.

three-body break-up of

The total absorption rate ~~$\pi^- + {}^3\mathrm{H} \to n + n + n$~~ is shown in Fig. 3.64 as a function of the chiral order of the SMS potential while each curve represents different cut-off values used to obtain the prediction. THe most advanced ~~configuration~~ was used in this case, namely Plane wave plus rescattering part, both single- and two-nucleon currents and two-nucleon plus three-nucleon ~~forces~~ interaction.

Similarly to the ~~process with~~ ^{3}He, we see that with each subsequent chiral order predictions become closer to each other, ~~so~~ the cut-off dependence gets weaker. Also, the prediction with $\Lambda = 550\,\mathrm{MeV}$ at N^{3}LO is strangely above the prediction with $\Lambda = 500\,\mathrm{MeV}$. We can also notice, that at N^{4}LO predictions with cut-off values 500 MeV and 550 MeV are much closer to each other than to ~~other values~~ results obtained with other Λs.

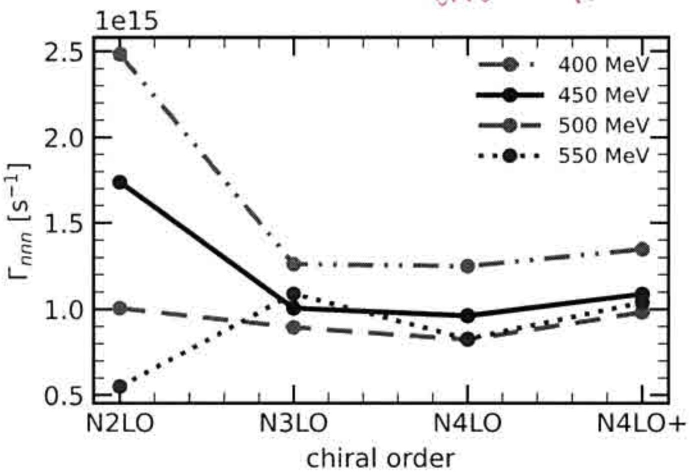

Figure 3.64: Absorption rate for $\pi^- + {}^3\mathrm{H} \to n + n + n$ reaction as a function of the chiral order with different values of the cut-off parameter Λ. Predictions were obtained with 3NF at N^{2}LO.

1. add remaining discussion of Figs 3.65 - 3.71

2 Both ~~[illegible]~~ In discussion for ^{3}He and ^{3}H I miss details which configuration is at specific (x, y)
For example, in our paper page 16: QFS(nn) is located at (x, y) = (0, 1). Please add such information to thesis
→ ~~[illegible]~~ take them from paper. That ~~[illegible]~~ will make paper more quantitative.

next page →

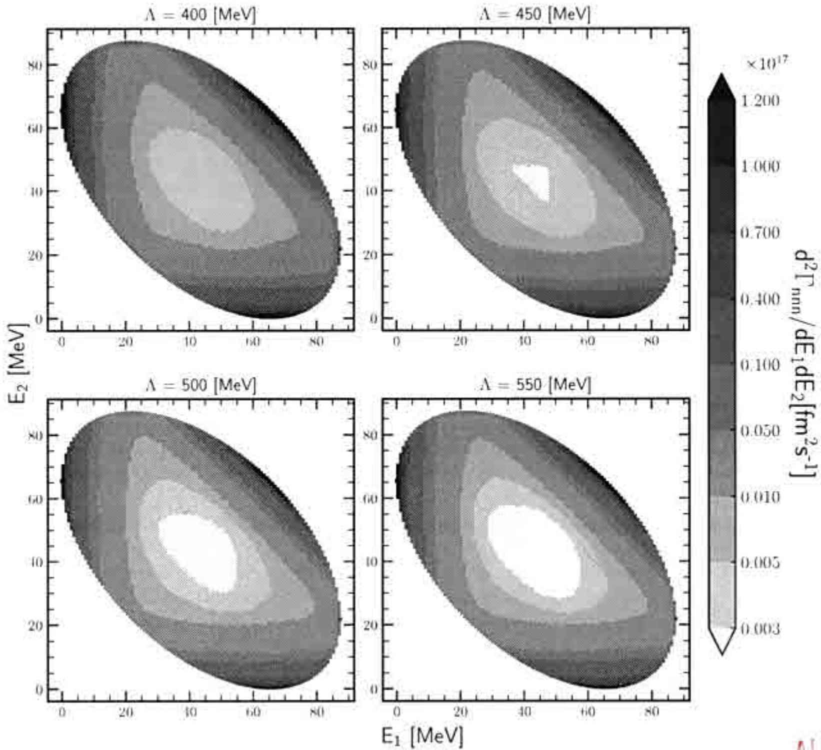

supplemented by N^2LO 3NF

ingredients

NN

Figure 3.65: Intensity plots for the double differential absorption rates $d^2\Gamma_{nnn}/dE_1dE_2$ for the $\pi^- +^3\mathrm{H} \rightarrow n + n + n$ process, obtained using the SMS potential at $\mathrm{N^4LO^+}$ with all ~~contributions~~ possible: plane wave + rescattering, 1NC + 2N, 2NF+3NF. Each panel presents predictions obtained with different values of the cut-off parameter Λ: from 400 MeV (upper left) to 550 MeV (lower right).

see Eq 4.10 - 4.16 from paper

3. At some point comparison with data (or info that there is no data) is needed. You can also mention comparison with Gotta et al (Tab V from the paper) + discussion. Also for 2?

4. Give numbers and description for total rates (~~totals~~ like Eq 4.10 - 4.12, 4.13, tab. 1 from paper)

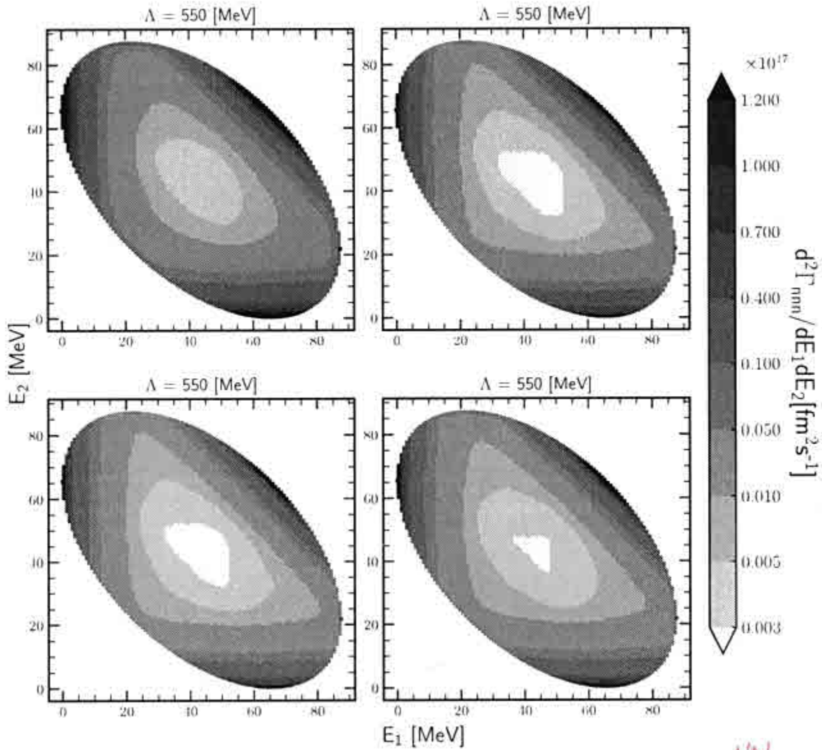

ingredients

NN

supplemented by the N²LO 3NF

Figure 3.67: Intensity plots for the double differential absorption rates $d^2\Gamma_{nnn}/dE_1dE_2$ for the $\pi^- + ^3\mathrm{H} \rightarrow n + n + n$ process, obtained using the SMS potential at N^{4}LO$^+$ with all ~~contributions~~ possible: plane wave – rescattering, 1NC – 2N, 2NF+3NF. Each panel present predictions obtained with different chiral orders of the SMS potential: from N^{2}LO (upper left) to N^{4}LO$^+$ (lower right) and with $\Lambda = 450\,\mathrm{MeV}$.

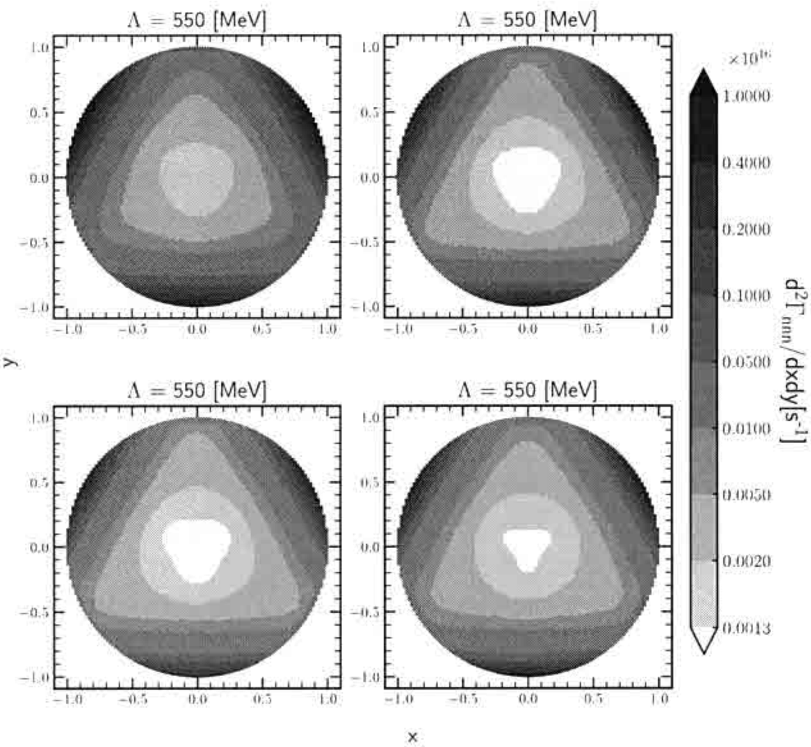

Figure 3.68: The same as in Fig. 3.67 but for the double differential absorption rates $d^2\Gamma_{nnn}/dxdy$.

The N^2LO 3NF was also used.

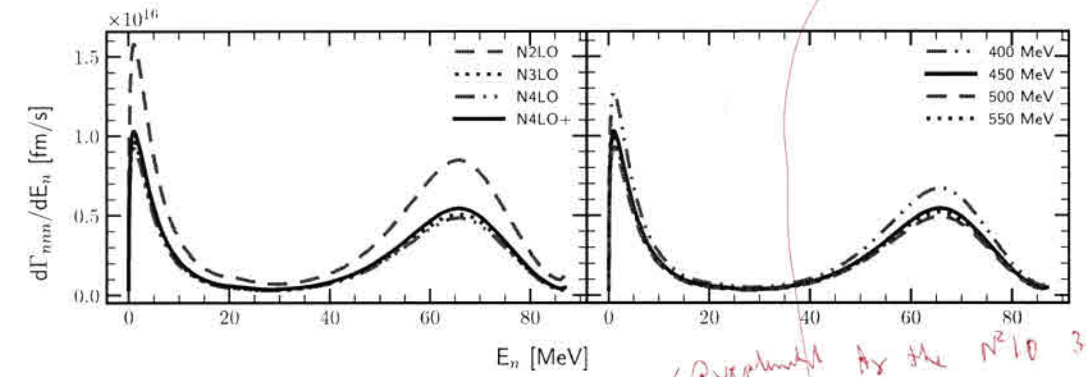

supplemented by the N^2LO 3NF

NN

with NN force at

Figure 3.69: Differential absorption rate $d\Gamma_{nnn}/dE_n$ as a function of the neutron energy E_n for the $\pi^- + 3H \rightarrow n + n + n$ process. Left panel shows results obtained ~~with~~ N^2LO (green dashed line), N^3LO (blue dotted line), N^4LO (red dashed-double-dotted line) and N^4LO^+ (black solid line) chiral orders, and with $\Lambda = 450$ MeV. The right panel includes results obtained with the N^4LO^+ SMS potential with different values of the Λ: 400 MeV (red dashed-double-dotted line), Λ: 450 MeV (black solid line), Λ: 500 MeV (green dashed line line) and Λ: 550 MeV (blue dotted line). All predictions were obtained with "FULL-(1NC+2N)-(2NF+3NF)" setup.

and only for pion absorption it was supplemented by two-nucleon current operator

For the ~~electromagnetic~~ photodisintegration I included two-body currents via the Siegert theorem

CHAPTER 4

SUMMARY

augmented by the consistently regularized ~~[illegible]~~ three-nucleon force at N²LO.

nucleon-nucleon

the semi-phenomenological

processes

In this thesis I investigated ^{2}H, ^{3}H and ^{3}He photodisintegrations as well as pion absorption by the same nuclei. In order to analyze these reactions and to calculate predictions for observables I used a chiral model of interaction namely the most advanced SMS chiral potential up to N^{4}LO$^+$ order. Results prepared with AV18 potential have been shown as a reference point. The current operator used is restricted to the single nucleon current

(1) → write

The ~~first~~ main goal of this work was to investigate ~~if the SMS potential is converged~~ with respect to the chiral order. It would then be a hint whether the development of higher ~~orders~~ order contributions to the potential is required. In most of the results ~~we~~ I observed a very converged predictions which was confirmed by a small difference between the last ~~two chiral~~ investigated orders: N^{4}LO and N^{4}LO$^+$. This difference in most of regarded ~~situations~~ cases ~~did~~ does not exceed a few percent. Another evidence is a width of the truncation band for N^{4}LO$^+$ predictions. For the deuteron photodisintegration process, observables have a ~~maximum width~~ truncation error always below 1 % for the ~~regarded~~ two studied photon energies ($E_\gamma = 30$ MeV and $E_\gamma = 100$ MeV). The same trend is presented also for other regarded reactions as well. This ~~hints~~ leads us towards a conclusion that further chiral orders would not improve the predictions much and current ~~potential~~ model ~~is~~ shows satisfactory converged~~ already~~ once. This is also confirmed by the AV18 predictions which are always very close to N^{4}LO$^+$ (see e.g. Fig. 3.8, Fig. 3.26 etc.).

(2) investigated

The other interesting point in the investigated chiral potential is its dependence on the value of ~~the cutoff parameter~~ its intrinsic cutoff parameter Λ, the four values of which (400, 450, 500 and 550 MeV) were investigated. ~~We~~ I have ~~observed~~ shown that the relative spread of predictions with respect to the cutoff value is higher for the ~~larger~~ higher energies. For example, the spread of the differential cross section for ^{3}He photodisintegration at $E_\gamma = 30$ MeV at the characteristic point (maximum) is around 3 %, while at $E_\gamma = 100$ MeV it is three times larger - around 3 % (see Fig. 3.28, Fig. 3.29 and discussions). Nevertheless, usually for higher energies the difference between the predictions obtained with different values of Λ is smaller than the difference with experimental data (when it is available) which is evidently visible in Fig. 3.5(b).

~~We~~ I have also ~~checked contributions from the various model components to~~ studied role of the various dynamical components of the model and by checking how they influence the predicted values. Namely, predictions obtained with plane wave part only (first term in the Eq. (2.31)), as well as predictions with and without 2N current contributions (~~obtained~~ introduced via the Siegert approach). For example, in the Fig. 3.4b we see predictions for the deuteron photodisintegration obtained without rescattering part (~~pink line~~), without 2N contributions (~~green line~~) and full predictions (~~blue line~~). Evidently the rescattering contribution of

I compare

with those ~~obtained~~ taking into account final state interactions

 cross section

(1) Both processes were studied in momentum space. ~~and th~~
The standard Lippmann-Schwinger equation is solved to get the t-operator and consequently 2N scattering state. For three-nucleon processes the formalism of Faddeev equations have been applied. I solved corresponding equations for Faddeev components both for the bound ~~3N~~ and scattering 3N states. In that way I include all initial state as well as final state interactions. I'm also able to test ~~the~~ importance of FSI by restricting computations to only plane wave approximation.

(2) ~~if the observables~~ ... to investigate a quality of currently available predictions ~~are~~ based on ~~the~~ the SMS interaction if applied to the studied here processes. Such information is necessary ~~in~~ due to expected two- and more-nucleon currents at ~~the~~ higher orders of chiral expansion, consistent with the SMS ~~...~~ potential. ~~Various aspects can be~~ Various features of the model can be studied in that context. Firstly, I ~~would like to~~ investigated if the predictions based on the SMS interaction are converged ...

The used formalism allows me to study not only the total cross section or capture rates but also various differential cross sections and polarization observables. That in turn allows me to conclude on sensitivity of various observables on studied effects and to pick up observables which after measurement could deliver valuable information.

predictions

relatively small

predicted cross sections

processes

~~part contribution~~ is relatively small for the $E_\gamma = 30\,\mathrm{MeV}$, but is increasing with larger energies. The analysis of the relative difference at the specific θ_p value does not show this trend (the differences are 10 %, 7 % and 4 % for $E_\gamma = 30$, 100 and 140 MeV respectively at $\theta_p = 80\,\%$), but we see that at the lower energy ~~curves~~ are qualitatively very similar and ~~the difference is~~ mainly around the maximum point~~(which is close to the analyzed point)~~. In contrast, for the larger energies, ~~curves~~ differ qualitatively and analyzed point is rather depicting the region were the difference is ~~minimal~~. The difference between the full predictions and the ones, where only 1NC was used is much ~~higher~~ bigger: even for the lowest energy ~~it is~~ around 50 % and for the larger two it grows up to $\sim 78\,\%$. ~~(at the same angle value)~~. Clearly, both rescattering part and 2NC contributions are very important and bring significant contribution. ~~The latter one is taken into account not completely, since there is no proper 2NC current available yet, but even using the Siegert approach proves that this part is very important in described process.~~ Similar trend is visible ~~at~~ also for other observables(see e.g. Fig. 3.10) and ~~other~~ processes (see Figs.3.52, 3.54, 3.56 to compare contributions for the pion absorption ~~at~~ on ^{3}He).

they differ

inclusion of two-body currents changes the cross section by

Giving mentioned above results, we can conclude that current version of the chiral potential is ~~good~~: it rather does not require any additional development in a sens of moving higher chiral orders or regularization, ~~but~~ 2NC is expected to bring a ~~large improvements to the predictions~~.

also

Our Full model nicely describes data up to $E_\gamma = 70\,\mathrm{MeV}$.

SMS

of very high quality

should be completely derived as it

~~Contrary~~ Contrary, the

significant contribution and thus improvements in our understanding of el-mag processes

That complex pattern ~~shows that~~ reveals interplay between ~~various~~ interaction and the current operator, and is one more recommendation after ~~deriving and~~ derivation of ~~application~~ ~~consist~~ fully consistent model, i.e. with consistent 2N forces, 3N forces and ~~and currents~~ one-, two- and three-body currents. Such model ~~should be~~ must be applied only within reliable scheme ~~to~~ compute observables. ~~My~~ work ~~is~~ culminated in the preparation of such scheme, both from analytical and numerical ~~aspects~~ sides, and now we are ready for study more sophisticated Hamiltonians.

(in points)

In summary you ~~are~~ should give few ~~p~~ detailed conclusions like

Among the studied processes and observables:

1) The most sensitive to FSI are for ... (observables, energies)

2) ―――――― " ―――――― 2NC

3) ―――――― " ―――――― 3NF

4) ~~cros~~ total cross section vs differential cross sections

5) cross sections vs polarization observables

6) Is it better do measurement on ^2H, ^3He or ^3H ?

7) stress that for $\pi + {}^3H$ there are three neutrons in final state which is very unusual but extremely interesting situation

8) For pion absorption write if you suggest measurements in FSI configuration, QFS or others ?

⋮

BIBLIOGRAPHY

[1] D. M. Skopik, Y. M. Shin, M. C. Phenneger, and J. J. Murphy. Photodisintegration of deuterium determined from the electrodisintegration process. *Phys. Rev. C*, 9:531–536, Feb 1974.

[2] F. F. Liu, D. E. Lundquist, and B. H. Wiik. Measurements of the polarization of protons from deuteron photodisintegration. *Phys. Rev.*, 165:1478–1482, Jan 1968.

[3] Reinhold Kose, Bjoern Martin, Rainer Runkel, Helmut Wahlen, and Karl Heinz Kissler. Measurements of the polarization of protons from deuteron photodisintegration for photon energies between 282 and 405 mev. *Zeitschrift für Physik A Hadrons and nuclei*, 220:305–320, 1969.

[4] T. Kamae, I. Arai, T. Fujii, H. Ikeda, N. Kajiura, S. Kawabata, K. Nakamura, K. Ogawa, H. Takeda, and Y. Watase. Observation of an anomalous structure in proton polarization from deuteron photodisintegration. *Phys. Rev. Lett.*, 38:468–471, Feb 1977.

[5] Andrew L. Cooper, K. J. Kelly, E. Machado, I. Pogrebnyak, J. Surbrook, C. Tysor, P. Thompson, M. Emamian, B. Walsh, B. Carlin, J. R. Dermigny, A. E. Champagne, and T. B. Clegg. Development of a variable-energy, high-intensity, pulsed-mode ion source for low-energy nuclear astrophysics studies. *Review of Scientific Instruments*, 89(8):083301, 2018.

[6] A.P. Tonchev, M. Boswell, C.R. Howell, H.J. Karwowski, J.H. Kelley, W. Tornow, and Y.K. Wu. The high intensity γ-ray source (hiγs) and recent results. *Nuclear Instruments and Methods in Physics Research Section B: Beam Interactions with Materials and Atoms*, 241(1):170–175, 2005. The Application of Accelerators in Research and Industry.

[7] J Bermuth, P Merle, C Carasco, D Baumann, R Böhm, D Bosnar, M Ding, M.O Distler, J Friedrich, J.M Friedrich, J Golak, W Glöckle, M Hauger, W Heil, P Jennewein, J Jourdan, H Kamada, A Klein, M Kohl, B Krusche, K.W Krygier, H Merkel, U Müller, R Neuhausen, A Nogga, Ch Normand, E Otten, Th Pospischil, M Potokar, D Rohe, H Schmieden, J Schmiedeskamp, M Seimetz, I Sick, S Širca, R Skibiński, G Testa, Th Walcher, G Warren, M Weis, H Witała, H Wöhrle, and M Zeier. The

[24] E. Epelbaum, W. Glöckle, and U.-G. Meißner. Improving the convergence of the chiral expansion for nuclear forces - i: Peripheral phases. *The European Physical Journal A*, 19(1):125–137, January 2004.

[25] P. Reinert, H. Krebs, and E. Epelbaum. Semilocal momentum-space regularized chiral two-nucleon potentials up to fifth order. *Eur. Phys. J.*, A54(5):86, 2018.

[26] E. Epelbaum. Few-nucleon forces and systems in chiral effective field theory. *Progress in Particle and Nuclear Physics*, 57(2):654–741, 2006.

[27] D. R. Entem, R. Machleidt, and Y. Nosyk. High-quality two-nucleon potentials up to fifth order of the chiral expansion. *Phys. Rev. C*, 96:024004, Aug 2017.

[28] E. Epelbaoum, W. Glöckle, and Ulf-G. Meißner. Nuclear forces from chiral lagrangians using the method of unitary transformation (i): Formalism. *Nuclear Physics A*, 637(1):107–134, 1998.

[29] E Epelbaum, W Glöckle, and UG Meißner. The two-nucleon system: Nuclear forces from chiral lagrangians using the method of unitary transformation ii. *Nucl. Phys. A*, 671:295–331, 2000.

[30] Evgeny Epelbaum, Walter Glöckle, and Ulf-G Meißner. The two-nucleon system at next-to-next-to-next-to-leading order. *Nuclear Physics A*, 747(2-4):362–424, 2005.

[31] R. Skibiński, J. Golak, K. Topolnicki, H. Witała, E. Epelbaum, W. Glöckle, H. Krebs, A. Nogga, and H. Kamada. Triton with long-range chiral n^3lo three-nucleon forces. *Phys. Rev. C*, 84:054005, Nov 2011.

[32] H Witała, J Golak, R Skibiński, and K Topolnicki. Calculations of three-nucleon reactions with n3lo chiral forces: achievements and challenges. *Journal of Physics G: Nuclear and Particle Physics*, 41(9):094011, jul 2014.

[33] E. Epelbaum, H. Krebs, and U. G. Meißner. Precision nucleon-nucleon potential at fifth order in the chiral expansion. *Phys. Rev. Lett.*, 115(12):122301, 2015.

[34] D. R. Entem and R. Machleidt. Accurate charge-dependent nucleon-nucleon potential at fourth order of chiral perturbation theory. *Phys. Rev. C*, 68:041001, Oct 2003.

[35] R Machleidt and D R Entem. Towards a consistent approach to nuclear structure: EFT of two- and many-body forces. *Journal of Physics G: Nuclear and Particle Physics*, 31(8):S1235–S1244, July 2005.

[36] R. Machleidt, P. Liu, D. R. Entem, and E. Ruiz Arriola. Renormalization of the leading-order chiral nucleon-nucleon interaction and bulk properties of nuclear matter. *Phys. Rev. C*, 81:024001, Feb 2010.

[37] M. Piarulli, L. Girlanda, L. E. Marcucci, S. Pastore, R. Schiavilla, and M. Viviani. Electromagnetic structure of A = 2 and 3 nuclei in chiral effective field theory. *Phys. Rev.*, C87(1):014006, 2013.

[38] M. Piarulli, L. Girlanda, R. Schiavilla, R. Navarro Pérez, J. E. Amaro, and E. Ruiz Arriola. Minimally nonlocal nucleon-nucleon potentials with chiral two-pion exchange including Δ resonances. *Phys. Rev. C*, 91:024003, Feb 2015.

[39] A. Ekström, G. R. Jansen, K. A. Wendt, G. Hagen, T. Papenbrock, B. D. Carlsson, C. Forssén, M. Hjorth-Jensen, P. Navrátil, and W. Nazarewicz. Accurate nuclear radii and binding energies from a chiral interaction. *Phys. Rev. C*, 91:051301, May 2015.

[40] Ingo Tews, Zohreh Davoudi, Andreas Ekström, Jason D Holt, and Joel E Lynn. New ideas in constraining nuclear forces. *Journal of Physics G: Nuclear and Particle Physics*, 47(10):103001, aug 2020.

[41] H.-W. Hammer, Sebastian König, and U. van Kolck. Nuclear effective field theory: Status and perspectives. *Rev. Mod. Phys.*, 92:025004, Jun 2020.

[42] Timo A. Lähde and Ulf-G. Meißner. *Nuclear Lattice Effective Field Theory*. Springer International Publishing, 2019.

[43] A. J. F. Siegert. Note on the interaction between nuclei and electromagnetic radiation. *Phys. Rev.*, 52:787–789, Oct 1937.

[44] J. Golak, H. Kamada, H. Witała, Walter Glöckle, J. Kuroś, R. Skibiński, V. V. Kotlyar, K. Sagara, and H. Akiyoshi. Faddeev calculations of proton deuteron radiative capture with exchange currents. *Phys. Rev.*, C62:054005, 2000.

[45] C.G.J. Jacobi. Ueber gauss neue methode, die werthe der integrale näherungsweise zu finden. 1826.

[46] C. Van Der Leun and C. Alderliesten. The deuteron binding energy. *Nuclear Physics A*, 380(2):261–269, 1982.

[47] W Glöckle. *The quantum mechanical few-body problem*. Texts and monographs in physics. Springer, Berlin, 1983.

[48] W. Glöckle, H. Witała, D. Hüber, H. Kamada, and J. Golak. The three-nucleon continuum: achievements, challenges and applications. *Physics Reports*, 274(3):107–285, 1996.

[49] R. Skibiński, J. Golak, H. Kamada, H. Witała, W. Glöckle, and A. Nogga. Search for three-nucleon force effects in two-body photodisintegration of ^{3}he(^{3}H) and in the time reversed proton-deuteron radiative capture process. *Phys. Rev. C*, 67:054001, May 2003.

[50] J Arrington, C D Roberts, and J M Zanotti. Nucleon electromagnetic form factors. *Journal of Physics G: Nuclear and Particle Physics*, 34(7):S23, may 2007.

[51] J. Jourdan. Measurements of neutron electromagnetic form factors. *Nuclear Physics A*, 654(1, Supplement 1):513c–516c, 1999.

[52] J. Golak, R. Skibiński, H. Witała, W. Glöckle, A. Nogga, and H. Kamada. Electron and photon scattering on three-nucleon bound states. *Phys. Rept.*, 415:89–205, 2005.

[53] Manfred Gari and W. Krümpelmann. The electromagnetic form factor of the neutron. *Physics Letters B*, 173(1):10–14, 1986.

[54] V. BERNARD, N. KAISER, and ULF-G. MEIßNER. Chiral dynamics in nucleons and nuclei. *International Journal of Modern Physics E*, 04(02):193–344, 1995.

[55] V. Lensky, V. Baru, J. Haidenbauer, C. Hanhart, A. E. Kudryavtsev, and U. G. Meißner. Towards a field theoretic understanding of NN $\rightarrow$ NNπ. *The European Physical Journal A*, 27(1):37–45, January 2006.

[56] J. Golak, R. Skibiśki, K. Topolnicki, H. Witała, A. Grassi, H. Kamada, and L. E. Marcucci. Momentum space treatment of inclusive neutrino scattering off the deuteron and trinucleons. *Phys. Rev.*, C98(1):015501, 2018.

[57] L. E. Marcucci, M. Piarulli, M. Viviani, L. Girlanda, A. Kievsky, S. Rosati, and R. Schiavilla. Muon capture on deuteron and ^{3}He. *Phys. Rev. C*, 83:014002, Jan 2011.

[58] D. Gotta, M. Dörr, W. Fetscher, G. Schmidt, H. Ullrich, G. Backenstoss, M. Izycki, W. Kowald, I. Schwanner, P. Weber, and H. J. Weyer. Negative pion absorption at rest in 3he. *Physical Review C*, 51(2):469–492, February 1995.

[59] E Epelbaum, H Krebs, and Ulf-G Meißner. Precision nucleon-nucleon potential at fifth order in the chiral expansion. *Phys. Rev. Lett.*, 115(12):122301, 2015.

[60] E Epelbaum, H Krebs, and U-G Meißner. Improved chiral nucleon-nucleon potential up to next-to-next-to-next-to-leading order. *Eur. Phys. J. A*, 51(5), May 2015.

[61] S. Binder, A. Calci, E. Epelbaum, R. J. Furnstahl, J. Golak, K. Hebeler, H. Kamada, H. Krebs, J. Langhammer, S. Liebig, P. Maris, Ulf-G. Meißner, D. Minossi, A. Nogga, H. Potter, R. Roth, R. Skibiński, K. Topolnicki, J. P. Vary, and H. Witała and. Few-nucleon systems with state-of-the-art chiral nucleon-nucleon forces. *Phys. Rev.*, C93(4):044002, 2016.

[62] Evgeny Epelbaum. High-precision nuclear forces : Where do we stand? *PoS*, CD2018:006, 2020.

[63] S. B. S. Miller, A. Ekström, and C. Forssén. Posterior predictive distributions of neutron-deuteron cross sections, 2022.

[64] J. A. Melendez, S. Wesolowski, and R. J. Furnstahl. Bayesian truncation errors in chiral effective field theory: Nucleon-nucleon observables. *Phys. Rev. C*, 96:024003, Aug 2017.

[65] R. Skibiński, J. Golak, K. Topolnicki, H. Witała, Yu. Volkotrub, H. Kamada, A. M. Shirokov, R. Okamoto, K. Suzuki, and J. P. Vary. Nucleon-deuteron scattering with the jisp16 potential. *Phys. Rev. C*, 97:014002, Jan 2018.

[66] Yu Volkotrub, J Golak, R Skibiński, K Topolnicki, H Witała, E Epelbaum, H Krebs, and P Reinert. Uncertainty of three-nucleon continuum observables arising from uncertainties of two-nucleon potential parameters. *Journal of Physics G: Nuclear and Particle Physics*, 47(10):104001, aug 2020.

[67] M. Bosman, A. Bol, J.F. Gilot, P. Leleux, P. Lipnik, and P. Macq. Measurement of the total cross section for the ^{1}H(n, γ) ^{2}H reaction between 37 and 72 mev. *Physics Letters B*, 82(2):212–215, 1979.

in photodisintegration of the deuteron by polarized. gamma. rays at low energies. *Sov. J. Nucl. Phys. (Engl. Transl.); (United States)*, 38:5, 11 1983.

[81] I E Vnukov, I V Glavanakov, Y F Krechetov, A P Potylitsyn, G A Saruev, V N Stibunov, and A N Tabachenko. Photodisintegration of the deuteron by linearly polarized photons below the pion-production threshold. *Sov. J. Nucl. Phys. (Engl. Transl.); (United States)*, 47:4, 4 1988.

[82] W. Del Bianco, L. Federici, G. Giordano, G. Matone, G. Pasquariello, P. Picozza, R. Caloi, L. Casano, M. P. De Pascale, L. Ingrosso, M. Mattioli, E. Poldi, C. Schaerf, P. Pelfer, D. Prosperi, S. Frullani, B. Girolami, and H. Jeremie. Neutron asymmetry measurements in the deuteron photodisintegration between 10 and 70 mev. *Phys. Rev. Lett.*, 47:1118–1120, Oct 1981.

[83] R. W. Jewell, W. John, J. E. Sherwood, and D. H. White. Polarization of photoneutrons produced from deuterium by 2.75-mev gamma rays. *Phys. Rev.*, 139:B71–B79, Jul 1965.

[84] J.M. Cameron, C.A. Davis, H. Fielding, P. Kitching, J. Pasos, J. Soukup, J. Uegaki, J. Wesick, H.S. Wilson, R. Abegg, D.A. Hutcheon, C.A. Miller, A.W. Stetz, and I.J. van Heerden. Radiative capture of polarized neutrons by hydrogen below the pion production threshold. *Nuclear Physics A*, 458(4):637–651, 1986.

[85] Th. Strauch, F. D. Amaro, D. F. Anagnostopoulos, P. Bühler, D. S. Covita, H. Gorke, D. Gotta, A. Gruber, A. Hirtl, P. Indelicato, E.-O. Le Bigot, M. Nekipelov, J. M. F. dos Santos, S. Schlesser, Ph. Schmid, L. M. Simons, M. Trassinelli, J. F. C. A. Veloso, and J. Zmeskal. Precision determination of the $d\pi \leftrightarrow$NN transition strength at threshold. *Phys. Rev. Lett.*, 104:142503, Apr 2010.

[86] Th. Strauch, F. D. Amaro, D. F. Anagnostopoulos, P. Bühler, D. S. Covita, H. Gorke, D. Gotta, A. Gruber, A. Hirtl, P. Indelicato, E. O. Le Bigot, M. Nekipelov, J. M. F. dos Santos, Ph. Schmid, S. Schlesser, L. M. Simons, M. Trassinelli, J. F. C. A. Veloso, and J. Zmeskal. Pionic deuterium. *The European Physical Journal A*, 47(7), July 2011.